Electronic Supplementary Material (ESI) for Physical Chemistry Chemical Physics.
This journal is © the Owner Societies 2015

Supporting Information

Coaxial Zn_2GeO_4@Carbon Nanowires Directly Grown on Cu Foils as High-Performance Anodes for Lithium Ion Batteries

Weimin Chen, Liyou Lu, Scott Maloney, Ying Yang, and Wenyong Wang*

Department of Physics and Astronomy, University of Wyoming, Laramie, WY 82071, USA

*E-mail: wwang5@uwyo.edu

Experimental method

Synthesis of h-Zn_2GeO_4 and h-Zn_2GeO_4@C. h-Zn_2GeO_4 nanowires were synthesized by a hydrothermal reaction.[1] GeO_2 (10 mmol) and $Zn(CH_3COO)_2 \cdot 2H_2O$ (10 mmol) were mixed in a solvent including 20 mL ethylenediamine and 10 mL deionized H_2O, and the mixture was kept in the oven at 180 ºC for 24 h. Carbon coating on the h-Zn_2GeO_4 nanowires was created by immersing them in a 0.5 M aqueous glucose solution for 24 h, followed by sintering the h-Zn_2GeO_4-glucose samples at 500 ºC in Ar gas for 2 h. The working electrode of h-Zn_2GeO_4 or h-Zn_2GeO_4@C was prepared using pre-fabricated h-Zn_2GeO_4 or h-Zn_2GeO_4@C nanowires with super P and polyvinylidene difluoride with a weight ratio of 8:1:1.

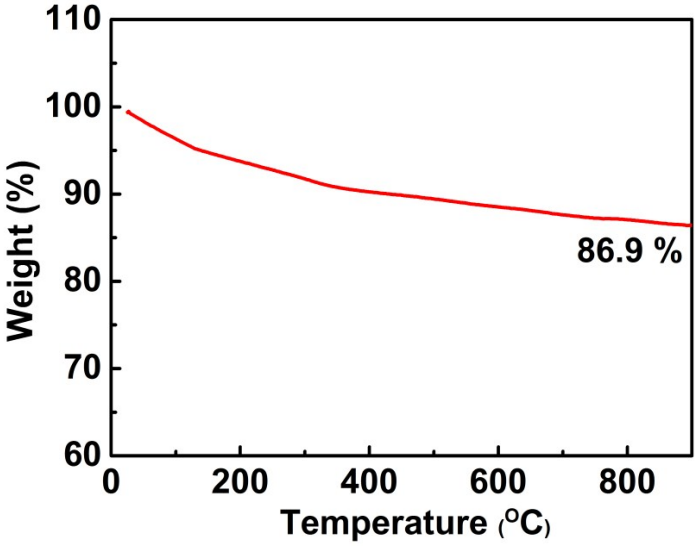

Figure S1. TGA curve of typical Zn_2GeO_4@C nanowires. The Zn_2GeO_4 content of nanowires estimated from the TGA is 86.9 %. The TGA data was collected in air with a heating rate of 10 ºC min^{-1}.

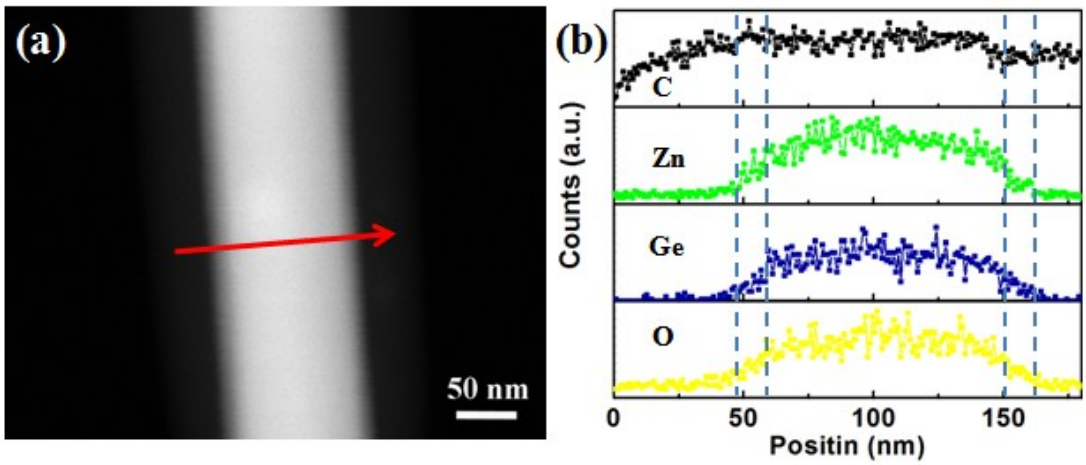

Figure S2. (a) Dark-field TEM image of the Zn_2GeO_4@C nanowire. (b) EDX line-scan element distributions of C, Zn, Ge and O along the line shown in (a).

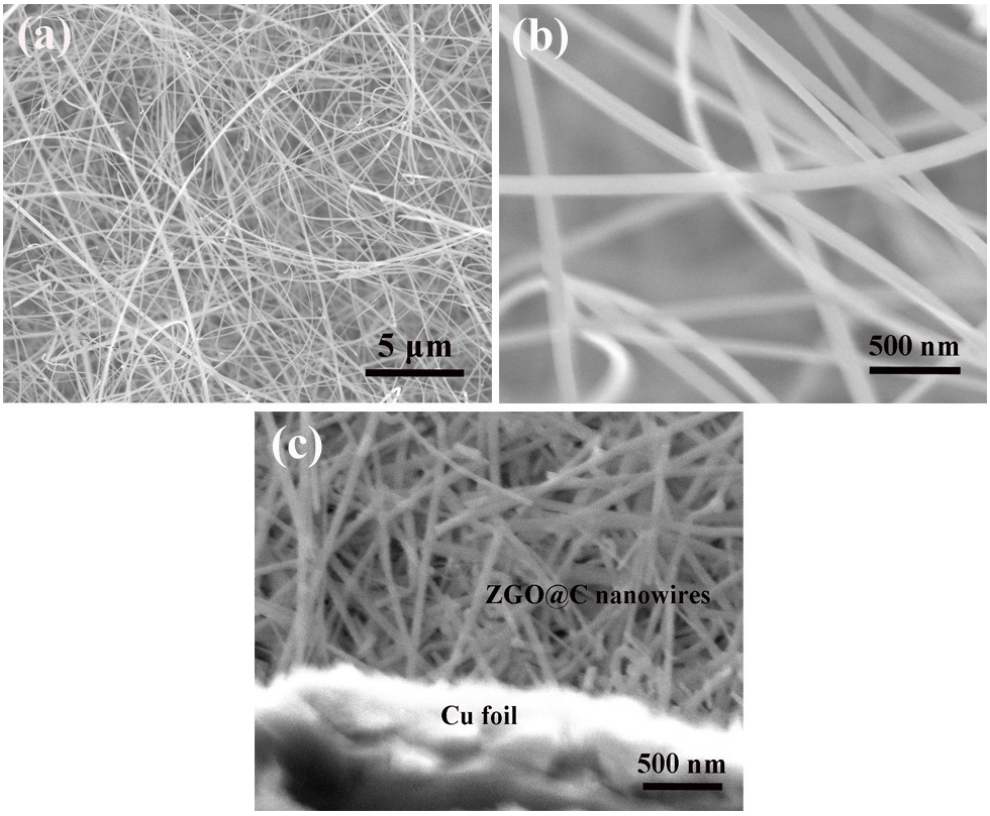

Figure S3. (a, b) SEM images of the ZGO@C nanowires. (c) Cross-sectional SEM image of ZGO@C nanowires on Cu foil. The nanowires showed arbitrary growth directions.

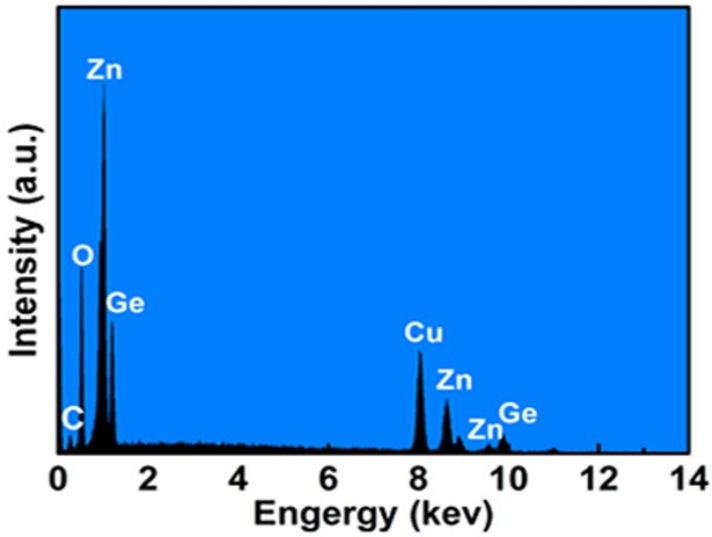

Figure S4. An EDX spectrum of a typical coaxial Zn_2GeO_4@C nanowire, which demonstrates the presence of Zn, Ge, O, and C in the structure. The Cu signals are from the Cu foil substrate.

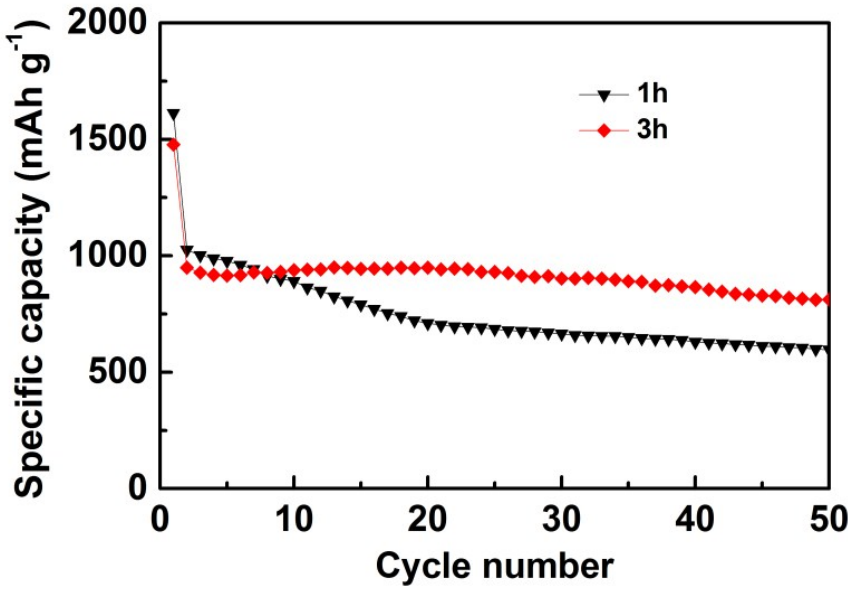

Figure S5. Cyclic performance of 1 h and 3 h ZGO@C/Cu electrodes at 0.2 A g^{-1}. After 50 cycles, the capacity of 1 h ZGO@C/Cu electrode decays quickly to 596 mAh g^{-1}, while the 3 h ZGO@C/Cu electrode is relatively stable and exhibits a capacity of 811 mAh g^{-1} after 50 cycles.

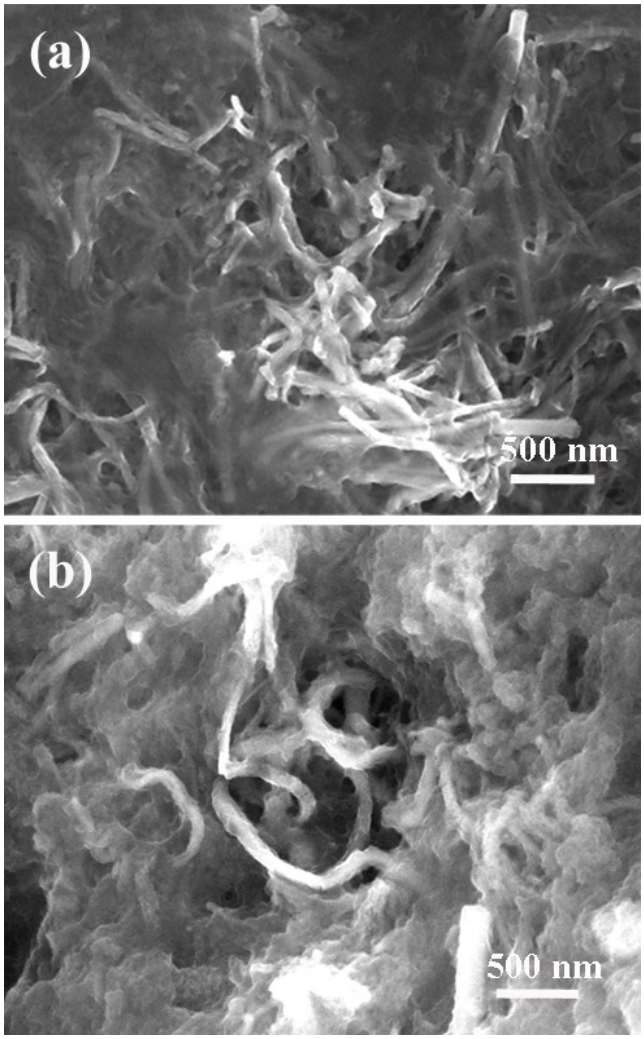

Figure S6. (a) SEM image of the ZGO@C/Cu electrode after 50-cycle test at 0.2 A g^{-1}. (b) SEM image of the ZGO@C/Cu electrode after 100-cycle test at 2.0 A g^{-1}. The images show that a SEI layer is formed on the surface of the Zn_2GeO_4@carbon nanowires.

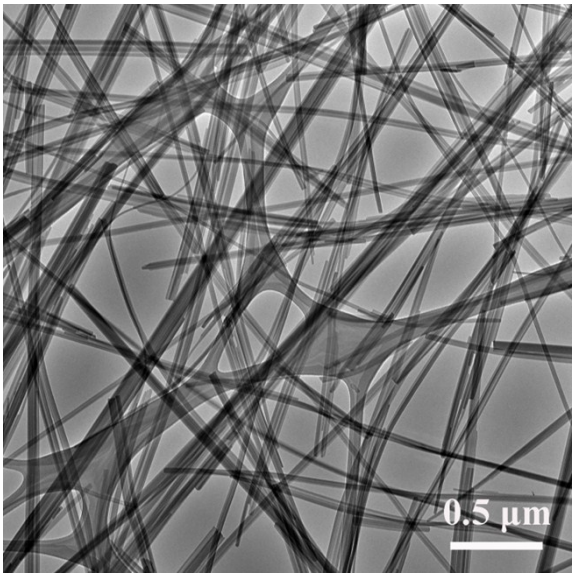

Figure S7. TEM image of h-Zn_2GeO_4 nanowires.

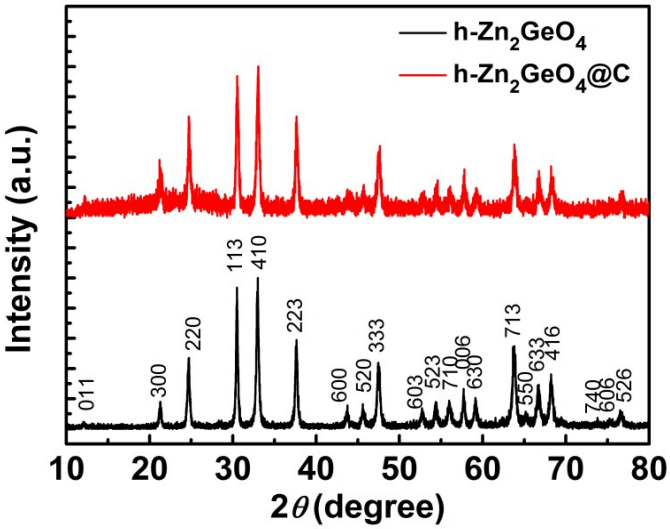

Figure S8. XRD spectra of h-Zn_2GeO_4 and h-Zn_2GeO_4@C nanowires. Both patterns fit well to the characteristic peaks of crystalline Zn_2GeO_4 (JCPDS card No. 11-0687).

Table S1 Comparison of electrochemical performance of Zn_2GeO_4-based or Zn-based ternary metal oxide LIB anodes

Materials	low Current density (A g^{-1})	Reversible Capacity (mAh g^{-1})	high Current density (A g^{-1})	Reversible Capacity (mAh g^{-1})	Reference
Zn_2GeO_4 nanorods	0.4	615	4.0	510	2
Zn_2GeO_4/N-doped graphene nanocomposites	0.1	1044	3.2	321	3
Zn_2GeO_4 nanoparticles	0.4	1250	6.4	470	4
Zn_2GeO_4/graphene oxide nanocomposites	0.2	1155	3.2	522	5
Zn_2GeO_4 nanorod/graphene composites	0.2	768	0.8	780	6
$ZnxCo_{3-x}O_4$ hollow polyhedra	0.1	990	9.0	575	7
$ZnMn_2O_4$/graphene nanosheets	0.5	800	3.2	568	8
Coaxial Zn_2GeO_4@carbon nanowires	0.2	1112	10.0	440	This work

Compared with previously published results of Zn_2GeO_4-based or Zn-based ternary metal oxide anodes, the ZGO@C/Cu electrode synthesized in this work exhibits higher capacity and stability at high-rate cycling.

References

1 Q. Liu, Y. Zhou, J. Kou, X. Chen, Z. Tian, J. Gao, S. Yan, Z. Zou, *J. Am. Chem. Soc.*, 2010, **132**, 14385–14387.

2 J. K. Feng, M. O. Lai, L. Lu, *Electrochem. Commun.*, 2011, **13**, 287−289.

3 F. Zou, X. L. Hu, Y. M. Sun, W. Luo, F. F. Xia, L. Qie, Y. Jiang, Y. H. Huang, *Chem.-Eur. J.*, 2013, **19**, 6027−6033.

4 R. Yi, J. Feng, D. Lv, M. L. Gordin, S. Chen, D. Choi, D. Wang, *Nano Energy*, 2013, **2**, 498−504.

5 F. Zou, X. L. Hu, L. Qie, Y. Jiang, X. Q. Xiong, Y. Qiao, Y. H. Huang, *Nanoscale*, 2014, **6**, 924−930.

6 R. Wang, S. Wu, Y. Lv, Z. Lin, *Langmuir*, 2014, **30**, 8215−8220.

7 R. Wu, X. Qian, K. Zhou, J. Wei, J. Lou, P. M. Ajayan, *ACS Nano*, 2014, **8**, 6297–6303.

8 P. Xiong, B. Liu, V. Teran, Y. Zhao, L. Peng, X. Wang, G. Yu, *ACS Nano*, 2014, **8**, 8610–8616.